Photoluminescence of nanodiamonds influenced by charge transfer from silicon and metal substrates

Stepan Stehlik, Lukas Ondic, Amanuel Berhane, Igor Aharonovich, Hugues Girard, Jean-Charles Arnault, Bohuslav Rezek

Photoluminescence of nanodiamonds influenced by charge transfer from silicon and metal substrates

Stepan Stehlik [a], Lukas Ondic [a], Amanuel M. Berhane [b], Igor Aharonovich [b], Hugues A. Girard [c], Jean-Charles Arnault [c], Bohuslav Rezek [a,d]

[a] Institute of Physics ASCR, Cukrovarnicka 10, 16200 Prague 6, Czech Republic

[b] School of Physics and Advanced Materials, University of Technology, Sydney, Australia

[c] Diamond Sensors Laboratory, CEA LIST, F-91191 Gif sur Yvette, France

[d] Faculty of Electrical Engineering, Czech Technical University, Technicka 2, 16627 Prague, Czech Republic

Abstract

Photoluminescence of 5 nm detonation nanodiamonds (DNDs) is studied as a function of their surface treatment (hydrogenation/oxidation) and underlying substrate materials (silicon, gold, platinum, and nickel). The substrates affect DND photoluminescence emission spectrum and lifetime in the spectral range of 600–800 nm. The dependence is different for hydrogenated and oxidized DNDs. We attribute these effects to different electrostatic charging of DNDs on the substrates with different work functions (4.4 to 5.5 eV). We discuss the data based on naturally present NV centers, their phonon sideband, and surface-related non-radiative transitions.

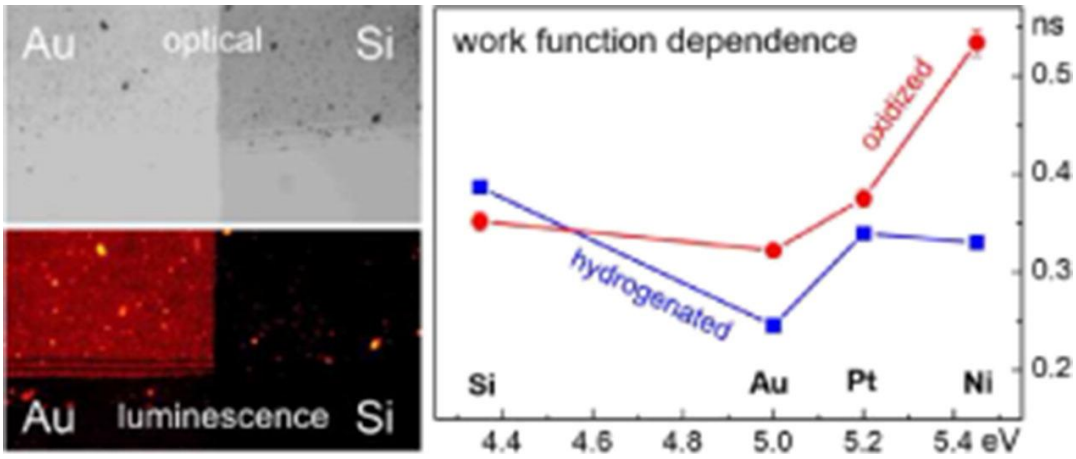

Keywords

Nanodiamonds, Photoluminescence, Electrostatic charging, Nanoparticles, Interfaces

1. Introduction

Nanodiamonds (NDs) belong to a family of carbon-based nanomaterials that are promising for numerous applications [1]. The most topical nowadays are applications of NDs in biology [2] such as imaging and drug delivery as well as in spintronics, photonics and quantum information technology [3], [4], [5]. The development of these applications gives rise to important progresses in surface modifications of nanodiamonds [6]. Photoluminescence (PL) is the key property in most of these applications. PL of nanodiamonds in visible spectral range can originate from dislocations and point defects [7], various color centers such as nitrogen or silicon vacancy centers (NV, SiV), and surface-related transitions in sp^2 carbon phase (often forming ND shell), surface defects, and surface chemical moieties [8], [9], [10], [11].

Photoluminescence of NDs is indeed to a great extent determined by the structure and chemistry of the surface due to considerable surface to volume ratio. For instance, ND surface termination was shown to control photoluminescence of NV centers. In particular, hydrogenation of NDs leads to quenching of luminescence related to negatively charged (NV^-) centers and as a result produced color shifts from

NV^- (638 nm) to neutral NV^0 (575 nm) photoluminescence [12]. Similarly, high quality surface oxidation [13] or fluorination (on both bulk diamond [14] and nanodiamonds on Pt substrate [15]) lead to enhancement of NV^- over NV^0 color center population compared to hydrogen-terminated diamonds.

Here we report another, novel effect that arises from the substrate the NDs reside on. Effect of substrate on electronic and PL properties of nanostructures such as graphene oxide [16] or MoS_2 [17] has been recently demonstrated. Similarly, we have demonstrated that NDs inherently accommodate their electrical potential to the substrate, resulting in up to 0.4 V different potential of the same nanoparticles on Au and Si substrates [18]. This effect was attributed to charge transfer and trapping on the nanoparticles which was dependent on the substrate material as well as on the surface termination of NDs. The effect was also independently confirmed by observation of different emission of secondary electrons in a scanning electron microscope (SEM). Here we show that the inherent charge transfer between NDs and substrate influences also photoluminescence of NDs in terms of PL spectral shifts and lifetimes. We also show that the PL changes depend on whether NDs are hydrogen or oxygen terminated and we discuss the data based on naturally present NV centers and their phonon sideband.

2. Experimental

As diamond nanoparticles we used detonation nanodiamonds (DNDs) provided by the NanoCarbon Research Institute Co., Ltd. (Japan) with nominal size of 5 nm. We compare hydrogenated (H-DNDs) and oxidized (O-DNDs) prepared by micro-wave enhanced plasma hydrogenation [19] or oxidation by air annealing [20]. The DNDs were dispersed in water by ultrasonication. The DNDs were de-agglomerated when dispersed in solution. The DLS, TEM and other basic characteristics of the employed DNDs are provided in our prior publication [18]. The colloidal dispersions were appropriately diluted in order to deposit only a thin layer of DNDs on the substrates by drop casting.

The substrates were n-type Si wafers (10 Ω cm) with various metals deposited (by sputtering or thermal evaporation) in the thickness of about 50 nm on top: Au, Pt, and Ni. The substrates provide a large range of surface work functions: Si 4.35 eV, Au 5.0 eV, Pt 5.2 eV, Ni 5.45 eV. We always combined two materials (from Si, Au, Pt, Ni) on one substrate for mutual reference.

For PL imaging we used an Olympus IX71 inverted optical microscope with 100 W mercury lamp (U-LH100HG) as the light source, WIGA fluorescence filter cube, and UPlanFL 20× objective [10]. The filter cube consisted of green excitation band pass filter (530–550 nm), red emission band pass filter (575–625 nm), and corresponding dichroic mirror. The exposure time was 20 s.

For measurements of PL spectra and time-resolved PL we used a custom built confocal fluorescence microscope using 514 nm green laser (~ 2 mW) for excitation through objective (100×, 0.7 NA) with confocal spot of about ~ 500 nm. Emitted PL was collected through a dichroic mirror, long pass filter and directed to an avalanche photo diode (APD) or a spectrometer [21].

3. Results

Fig. 1 shows optical and fluorescence images of H-DNDs measured at Au/Si and Ni/Pt boundary. Optical images in Fig. 1a and c show that the surface is coated mostly by a thin DND layer (thickness 20–50 nm estimated by atomic force microscopy). Dark dots correspond to large DND clusters arising from the deposition process. Thus the fluorescence originates mostly from DND clusters and not from single particles. Yet note that as the DNDs were de-agglomerated in the solution the DND clusters on the surface are composed of truly single particles bound by Van der Waals forces. This is thus different to the typical DND agglomerates in detonation soot (referred to as core agglutinates). To obtain background reference from the substrate the DND layer was partially removed from the substrate mechanically along a horizontal direction. This region is visible as brighter stripe in the optical images in Fig. 1a and c.

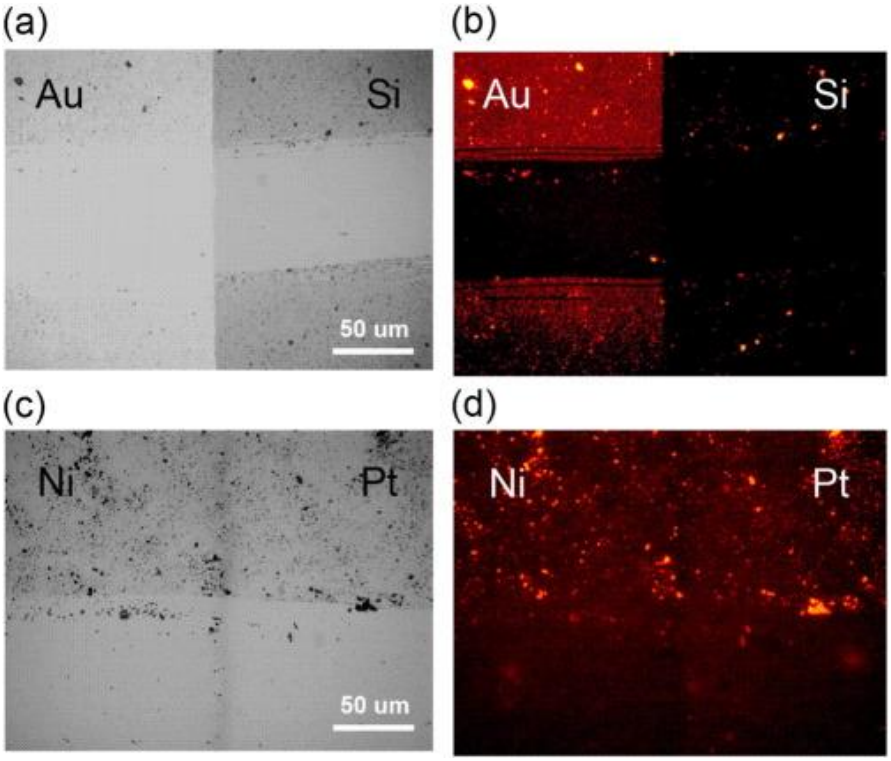

Fig. 1. Optical (a, c) and fluorescence microscope images (b, d) of H-terminated DNDs measured at Au/Si and Ni/Pt boundary. The DND layer is partially removed from the substrate mechanically along horizontal direction to provide the background reference.

Corresponding fluorescence images in Fig. 1b and d show that there is a large difference in PL intensity of H-DNDs on the Au and Si substrate: H-DNDs on Si exhibit 2% of the PL intensity they exhibit on Au (intensity averaged in the area of 30 × 30 μm^2). On the other hand, there is no noticeable difference between PL on Ni and Pt substrates. Thus it is not the difference in substrate work function and corresponding different charge of the nanoparticles that control the overall PL intensity. The most likely reason is difference in the substrate reflectivity. As can be seen in optical images, Ni and Pt exhibit similar reflectivity while Au reflects more light than Si. This is well correlated with the observed PL intensity. At the same settings, O-DNDs showed much weaker PL intensity, difficult to detect vs. background (images not shown).

On the other hand, PL spectra in Fig. 2 show broad PL band around 700 nm that shifts in dependence on the substrate material. Note that the spectra in Fig. 2 were normalized due to different PL intensities on different substrates and on differently terminated nanodiamonds. For O-DNDs (Fig. 2a) the PL maximum remains about the same for Si and Au at 680 nm while for Ni it shifts to about 700 nm. The trend is different for H-DNDs. Fig. 2b shows that PL maximum is about the same at 660 nm for Si and Ni while it shifts to 640 nm for the Au substrate. In both cases the difference is about 20 nm. The PL shift thus depends on the work function of the substrate with a non-uniform trend. We measured time-resolved PL to obtain more insight into the kinetics of photo-generated charges in DNDs on various substrates.

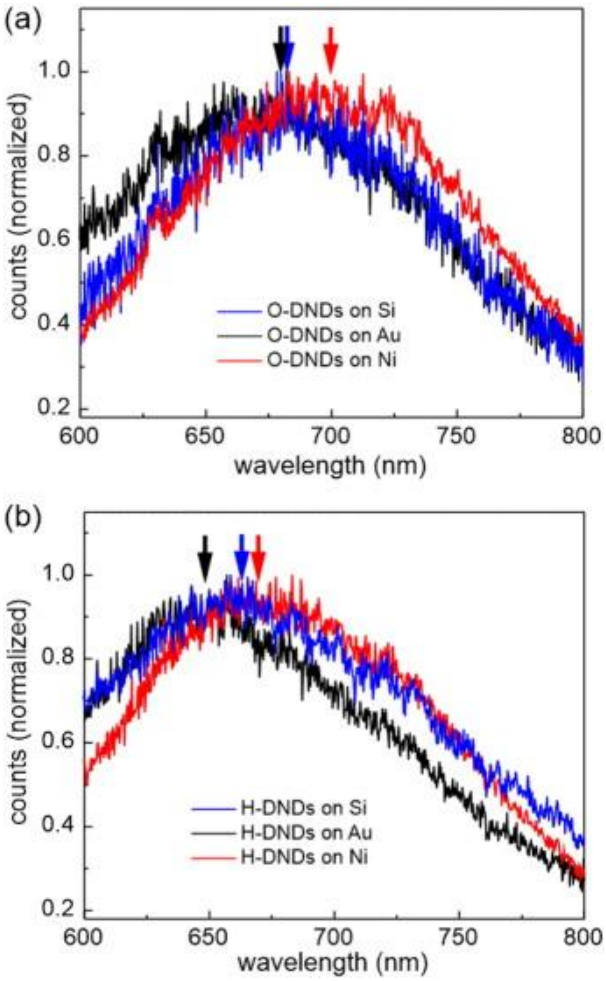

Fig. 2. Steady state photoluminescence spectra (PL excitation at 514 nm) of O-DNDs (a) and H-DNDs (b) on Si, Au, and Ni substrates. The spectra were normalized due to different PL intensities on different substrates and on differently terminated nanodiamonds.

Fig. 3 shows examples of PL decay profiles of H-DNDs and O-DNDs on Au and Ni. The presented PL decay profiles are typical and they are well reproducible across the sample. The decays were measured as integrated PL intensity after the excitation by picosecond laser at 514 nm. PL decays were measured on all the substrates; we only selected the two for better clarity of presentation. They were chosen as there was the most pronounced effect on PL spectrum observed for both H-DNDs and O-DNDs. One can see that Ni leads to slower PL decay on both H-DNDs and O-DNDs compared to Au.

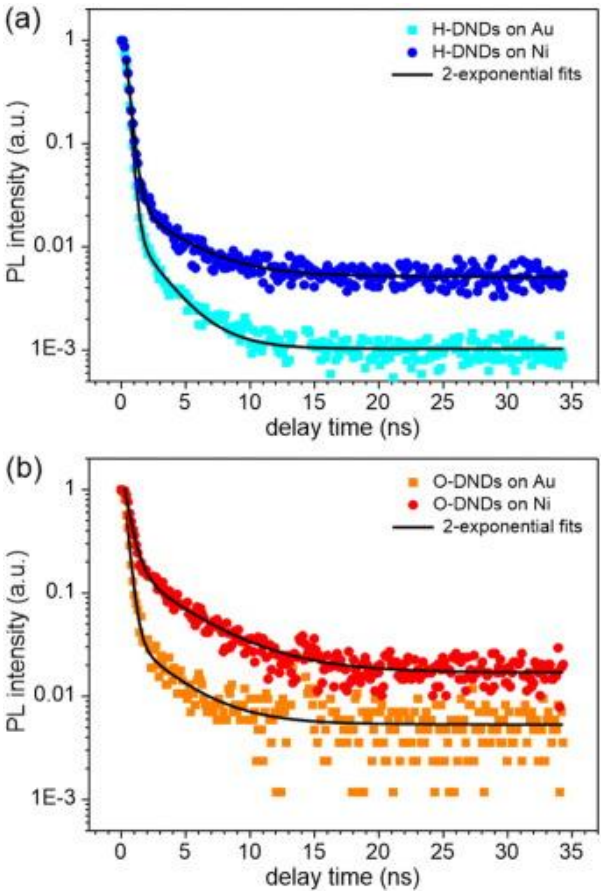

Fig. 3. Integrated PL decay profiles of H-DNDs (a) and O-DNDs (b) on Au and Ni. PL excitation was at 514 nm. Fits by double exponential function are indicated by the black line.

To evaluate the PL decays we fitted the data by the double exponential function $A(t) = A1 * \exp.(-t / t1) + A2 * \exp.(-t / t2)$, where *t1* and *t2* are characteristic fast and slow components of the fluorescence decay profile and *A1* and *A2* are their respective coefficients. The fit is indicated by the black line for each data set. The double exponential fitted the data accurately in all cases, including the data on other substrates. Let us note that also a stretched exponential function can be used to fit the PL decay, however, it provided much larger fitting error than the double exponential fits.

Fig. 4 summarizes the values of fast (*t1*) and slow (*t2*) PL decay times (lifetimes) as obtained from the double exponential fits for all the substrates. Where the error bar is not visible, it is smaller than the data symbol. The fast component is in the order of 0.1 ns (more precisely in the range of 0.2–0.6 ns) while the slow component is in the order of 1 ns (more precisely in the range of 2.3–4.3 ns). The faster process dominates all the decay characteristics of both H-DNDs and O-DNDs (prefactor ratio *A1*/*A2* always > 1).

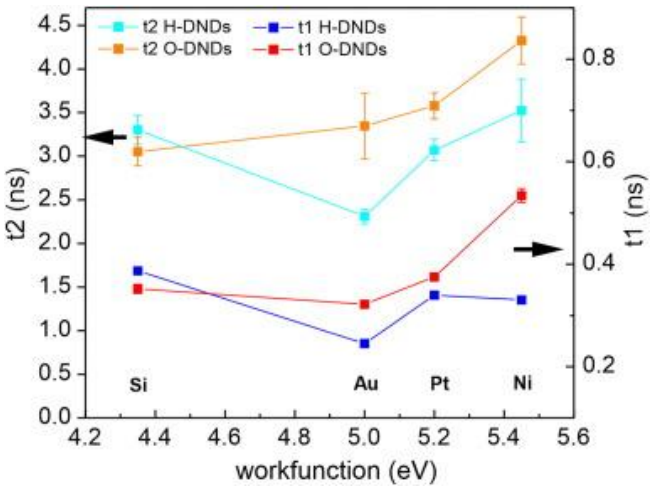

Fig. 4. Values of fast (*t1*) and slow (*t2*) PL decay times obtained from the double exponential fits and plotted as a function of substrate work function for H-DNDs and O-DNDs.

The decay times are plotted as a function of the substrate work function. We can see that the trend in short and fast decay times is similar for particular DNDs. On the other hand there is a pronounced difference in the trend for H-DNDs and O-DNDs.

Decay times of O-DNDs exhibit more or less monotonous trend. The decay times remain almost the same between Si and Au, then they start to rise towards higher work functions from Au to Ni. On the other hand, decay times of H-DNDs exhibit a minimum on Au and increase towards lower work functions (Si) and higher work functions (Ni).

4. Discussion

4.1. Discussion of PL spectra

Broad band PL of nanodiamonds can generally span from 500 nm to 800 nm in dependence on particle size and excitation wavelength [22]. Such broadband PL typically originates from volume dislocations and point defects or from surface defects, sp^2 carbon phase, and surface chemical moieties. So-called A-band of volume defects is typically at around 430 nm, i.e. in blue spectral region [7]. Recent study of surface chemistry-dependent PL study on nanodiamonds observed a blue PL component (around 430 nm) that was assigned to –OH bonds while green peak (around 520 nm) was attributed to –COOH and C–O–C groups [11]. Typical PL broadband between 400–600 nm is observed also on nanocrystalline diamond with sp^2 phase between and on the nanocrystal surfaces [9].

However, unlike surface and defect related PL spectra discussed above, the broadband PL emission peaks at 640–700 nm in our case. The PL spectrum of O-DNDs around 700 nm resembles negatively charged NV^- center including a weak emission peak at 637 nm [15], [23]. It was consistently observed on all O-DNDs. The PL band is blue shifted on H-DNDs and the peak at 637 nm (likely corresponding to NV^-) is missing. This is in agreement with the literature on NV centers where oxidation leads to increased NV^- intensity at the expense of NV^0 center [12], [13]. We do not have an unambiguous proof that the luminescence originates from NV centers. Nevertheless, the presence of typical phonon sideband and a small, yet reproducible hint of the NV^- peak is an indication of NV presence. Thus the observed PL is most likely related to NV centers, where the broadband PL corresponds to phonon sideband of the NV center emission, not to surface-related defects as suggested previously [24].

This is somewhat surprising on pristine, 5 nm small detonation nanodiamonds without any specific treatment for NV fabrication. There were concerns that photostable luminescent NV centers do not exist in 5-nm diamonds and so far only few studies (on intentionally embedded NV centers) indicated otherwise [24]. Nevertheless, it corroborates a previous indication that such NV-related PL without special treatment is possible [22]. It is also in perfect agreement with the 50 nm shift of the PL broadband to longer wavelengths from H-DNDs to O-DNDs. Similar phonon sideband shift has been

observed for oxidation [13] as well as for fluorination [15] of bulk and nano diamonds with the intentionally created NV centers.

This also means that the NV centers are inherently very close to the DND surface. The NV-related PL is thus more prone to be affected by condition of the surface and nearby surroundings. Fig. 2 showed that the phonon sideband spectrum was indeed clearly influenced by the substrate material (up to 20 nm shifts) for both H-DNDs and O-DNDs. On the other hand, NV^- position (zero phonon line) was not influenced.

4.2. Discussion of PL lifetimes

Time-resolved PL provided further information on the PL mechanism and influence of the substrate material. In all the cases, PL decays of both H-DNDs and O-DNDs were best fitted by double exponential function with two decay times (lifetimes). Double exponential corresponds to two independent PL processes, faster and slower one. Nevertheless, both processes have exponential decay thus they correspond to similar radiative recombination mechanism.

Usually, NV PL is modeled as a three-level system, two main levels and a metastable state [25]. Thus the two decay times can be attributed to the direct transition and delayed transition due to temporary residence in the metastable state. It should be noted that only a single exponential decay has been shown in many prior works [26]. Thus in our case the visibility of the two processes must be somehow related with the small DND size and naturally present NV centers. This would be in agreement with some prior indications of multi-exponential decays in NDs below 10 nm size [24]. It is noticeable that both decay times exhibit same trend as function of the substrate work function. Both types of transitions (including their phonon sideband) are thus influenced by the substrate in terms of lifetime.

The obtained PL decay times (~ 0.1–1 ns) are much shorter than typical PL lifetimes of NV color centers (~ 10–100 ns). Shortening of NV center lifetimes is generally possible. It has been shown that NV lifetime can depend on the NV distance from the substrate [26]. In addition, it can be reduced by modifying the refractive index of the environment surrounding the nanodiamonds [26]. But the reduction was only by 63% on average, not by an order of magnitude as in our case. It was also reported that PL lifetime of NV^- centers embedded within a cavity in the strong Purcell regime can be in principle reduced to tens of picoseconds [27]. In our case the DNDs are not in and do not form a resonating photonic cavity. Even if they would the PL lifetime shortening would be only in a narrow spectral range. Nevertheless, the articles above evidenced fundamental feasibility of even shorter PL decay times than observed here.

In our case, the shorter PL decay times are most likely related with existence of surface states on DNDs. Unlike many previous studies on larger nanodiamonds (typically > 20 nm), the NV centers are inherently very close to the surface and the surface plays much larger role due to considerable surface to volume ratio (~ 15% on 5 nm DNDs) in our case. Thus it is likely that the PL decays are shortened by surface-related non-radiative transitions, a general and well known effect in photoluminescence. In other words, the photogenerated carriers get trapped on the surface (or defect states in the bulk). Another possibility may be electron–phonon coupling that for nanodiamonds can take significant values and has mode frequencies in the THz (i.e. picosecond) range [28]. By electron–phonon coupling, relaxation of excitons in nanostructures can be significantly enhanced and it can reduce lifetimes below a nanosecond [29]. Exact pathway of the short PL decay in DNDs is not yet completely clear. Nevertheless it does not hinder discussion of the substrate effects on nanodiamonds PL.

4.3. Discussion of substrate effects

From the obtained data it is obvious that the PL spectra and both PL lifetimes of DNDs indeed depend on the substrate material. Since the DNDs are only about 5 nm in diameter, it means that there are about 4–10 layers of DNDs stacked on the surface. At the moment we may only speculate how all these particles feel the substrate, e.g. via semiconducting properties of DNDs (insulating core, conductive sp^2 shell or H-terminated surface, etc.). Nevertheless, we already proved by Kelvin probe force microscopy (KPFM) that electrical potential of nanodiamond deposits of such height is indeed accommodated to the substrate, thus the DNDs are charged as much as 0.4 V even in such thickness

[18]. This has been corroborated also by SEM in the same work as well as by intentional charging in another work [30]. Thus we believe that it is reasonable to assume also effects on PL emission in such thickness.

There are two possible mechanisms: i) charge transfer from photo-generated excitons from DNDs to substrate and ii) trapped charge on DNDs due to work function difference. Charge transfer from excitons in DNDs is unlikely as it is typically associated with power law PL decay [9]. Influence of charge trapping is much more likely though. Large dipole moment of NV means that the center is extremely sensitive to strain and mobile charges [31]. Shortened PL decays also corroborate involvement of charge trapping at surface or defect states. Different charging of H-terminated, oxidized, and partially graphitized DNDs due to different substrate materials as well as due to intentionally applied voltage was evidenced by Kelvin probe microscopy [30]. The charge may be thus predominantly retained in diamond surface states (including states arising due to surface oxidation, imperfect hydrogen termination, sp^2 phase and dangling bonds) as indicated by microscopic and electronic transport studies [32], [33].

The persistent electrostatic charging of DNDs can thus explain different PL decay times as well as PL spectral shifts. For explaining the different work function trends of H-DNDs and O-DNDs PL decay times we suggest the following model. Different work functions of the employed substrates give rise to variations in contact potential differences (CPD) between the DNDs and substrates and to different alignments of energetic levels in the DNDs and substrates.

In the case of H-DNDs, there is minimal CPD on Au due to the lowest work function difference between Au and H-terminated diamond as observed on bulk diamond [34]. As the work function increases or decreases the charging of DNDs increases and decay times increase correspondingly. Important point is that Fermi level is not pinned on H-terminated diamond and thus it can move freely as the interface changes [35].

In the case of O-DNDs, the steady trend from Si to Au and rising trend from Au to Ni could be explained by matching with the energetic level of surface states on oxidized diamond [36], [37]. The surface states on oxidized diamond are reportedly about 5 eV below vacuum level (precise value may change slightly depending on crystallographic orientation and oxidation procedure). Thus holes can be trapped in these surface states for higher substrate work functions, i.e. for Pt or Ni. For lower work functions the charge exchange is not in effect as holes are not easily discharged from these surface states [32].

5. Conclusions

The presented PL spectra and PL decay data evidenced novel effect of substrate on PL of DNDs. Broadband PL at 600–800 nm was attributed the phonon sideband of naturally present NV color centers. The fluorescence microscope showed clear differences in PL intensity of the same DNDs on different substrates. However, this was mainly due to different reflectivity of the substrates. On the other hand, the PL spectra shifts (by about 20 nm) and changes of PL decay times (by as much as 50%) show clear influence of the substrate work function within the range of 4.4 to 5.5 eV. Actual PL mechanism has not changed as all the PL decays were all fitted well by double exponential function. The substrate effect on PL was attributed to electrostatic charging of DNDs from substrate, which was evidenced before by KPFM and SEM as an inherent phenomenon. The electrostatic charge is assumed to be retained in sp^2 phase and surface states on DNDs. While this is a general mechanism, there were noticeable differences between H-DNDs and O-DNDs when the trends were plotted as a function of substrate work function. We proposed a model based on alignment of energetic states at DND/substrate junction, in similarity to bulk diamond properties. These results may be important for applications of DNDs in imaging, sensing, and quantum information as well as for fundamental understanding of PL emission processes in DNDs.

Prime novelty statement

Here we show that the inherent charge transfer between detonation nanodiamonds (DNDs) and substrates with different workfunction influences photoluminescence of DNDs in terms of PL spectral shifts and lifetimes. We also show that the PL changes depend on whether DNDs are hydrogen or

oxygen terminated and we discuss the data based on naturally present NV centers and their phonon sideband.

Acknowledgments

This work was supported by the GACR research project 15-01809S (BR, SS). It occurred in the frame of the LNSM infrastructure. I.A. is the recipient of an Australian Research Council Discovery Early Career Research Award (Project No. DE130100592).

References

[1] V.N. Mochalin, O. Shenderova, D. Ho, Y. Gogotsi. The properties and applications of nanodiamonds. Nat. Nanotechnol., 7 (2012), pp. 11-23, 10.1038/nnano.2011.209

[2] A.M. Schrand, S.A.C. Hens, O.A. Shenderova. Nanodiamond particles: properties and perspectives for bioapplications. Crit. Rev. Solid State Mater. Sci., 34 (2009), pp. 18-74, 10.1080/10408430902831987

[3] I. Aharonovich, E. Neu. Diamond nanophotonics. Adv. Opt. Mater., 2 (2014), pp. 911-928, 10.1002/adom.201400189

[4] M. Geiselmann, R. Marty, F.J. García de Abajo, R. Quidant. Fast optical modulation of the fluorescence from a single nitrogen-vacancy centre. Nat. Phys., 9 (2013), pp. 785-789, 10.1038/nphys2770

[5] J. Tisler, G. Balasubramanian, B. Naydenov, R. Kolesov, B. Grotz, R. Reuter, *et al.* Fluorescence and spin properties of defects in single digit nanodiamonds. ACS Nano, 3 (2009), pp. 1959-1965, 10.1021/nn9003617

[6] J.C. Arnault. Surface modifications of nanodiamonds and current issues for their biomedical applications. N. Yang (Ed.), Nov. Asp. Diam., Springer International Publishing (2015), pp. 85-122. http://link.springer.com/chapter/10.1007/978-3-319-09834-0_4 (accessed June 26, 2015)

[7] W.D. Partlow, J. Ruan, R.E. Witkowski, W.J. Choyke, D.S. Knight. Cryogenic cathodoluminescence of plasma-deposited polycrystalline diamond coatings. J. Appl. Phys., 67 (1990), pp. 7019-7025, 10.1063/1.345048

[8] F. De Weerdt, A.T. Collins. Broad-band luminescence in natural brown type Ia diamonds. Diam. Relat. Mater., 16 (2007), pp. 512-516, 10.1016/j.diamond.2006.10.003

[9] P. Galář, J. Čermák, P. Malý, A. Kromka, B. Rezek. Electrochemically grafted polypyrrole changes photoluminescence of electronic states inside nanocrystalline diamond. J. Appl. Phys., 116 (2014), p. 223103, 10.1063/1.4903937

[10] L. Ondič, K. Dohnalová, M. Ledinský, A. Kromka, O. Babchenko, B. Rezek. Effective extraction of photoluminescence from a diamond layer with a photonic crystal. ACS Nano, 5 (2011), pp. 346-350, 10.1021/nn1021555

[11] J. Xiao, P. Liu, L. Li, G. Yang. Fluorescence origin of nanodiamonds. J. Phys. Chem. C, 119 (2015), pp. 2239-2248, 10.1021/jp512188x

[12] V. Petráková, A. Taylor, I. Kratochvílová, F. Fendrych, J. Vacík, J. Kučka, *et al.* Luminescence of nanodiamond driven by atomic functionalization: towards novel detection principles. Adv. Funct. Mater., 22 (2012), pp. 812-819, 10.1002/adfm.201101936

[13] K.-M.C. Fu, C. Santori, P.E. Barclay, R.G. Beausoleil. Conversion of neutral nitrogen-vacancy centers to negatively charged nitrogen-vacancy centers through selective oxidation. Appl. Phys. Lett., 96 (2010), p. 121907, 10.1063/1.3364135

[14] S. Cui, E.L. Hu. Increased negatively charged nitrogen-vacancy centers in fluorinated diamond. Appl. Phys. Lett., 103 (2013), p. 051603, 10.1063/1.4817651

[15] T.W. Shanley, A.A. Martin, I. Aharonovich, M. Toth. Localized chemical switching of the charge state of nitrogen-vacancy luminescence centers in diamond. Appl. Phys. Lett., 105 (2014), p. 063103, 10.1063/1.4883229

[16] J.R. Rani, J. Lim, J. Oh, D. Kim, D. Lee, J.-W. Kim, *et al.* Substrate and buffer layer effect on the structural and optical properties of graphene oxide thin films. RSC Adv., 3 (2013), pp. 5926-5936, 10.1039/C3RA00028A

[17] M. Buscema, G.A. Steele, H.S.J. van der Zant, A. Castellanos-Gomez. The effect of the substrate on the Raman and photoluminescence emission of single-layer MoS2. Nano Res., 7 (2015), pp. 561-571, 10.1007/s12274-014-0424-0

[18] S. Stehlik, T. Petit, H.A. Girard, J.-C. Arnault, A. Kromka, B. Rezek. Nanoparticles assume electrical potential according to substrate, size, and surface termination. Langmuir, 29 (2013), pp. 1634-1641, 10.1021/la304472w

[19] H.A. Girard, J.C. Arnault, S. Perruchas, S. Saada, T. Gacoin, J.-P. Boilot, *et al.* Hydrogenation of nanodiamonds using MPCVD: a new route toward organic functionalization. Diam. Relat. Mater., 19 (2010), pp. 1117-1123, 10.1016/j.diamond.2010.03.019

[20] H. Kozak, Z. Remes, J. Houdkova, S. Stehlik, A. Kromka, B. Rezek. Chemical modifications and stability of diamond nanoparticles resolved by infrared spectroscopy and Kelvin force microscopy. J. Nanoparticle Res., 15 (2013), pp. 1-9, 10.1007/s11051-013-1568-7

[21] K. Bray, R. Previdi, B.C. Gibson, O. Shimoni, I. Aharonovich. Enhanced photoluminescence from single nitrogen-vacancy defects in nanodiamonds coated with phenol-ionic complexes. Nanoscale., 7 (2015), pp. 4869-4874, 10.1039/C4NR07510B

[22] P.-H. Chung, E. Perevedentseva, C.-L. Cheng. The particle size-dependent photoluminescence of nanodiamonds. Surf. Sci., 601 (2007), pp. 3866-3870, 10.1016/j.susc.2007.04.150

[23] C. Bradac, T. Gaebel, N. Naidoo, M.J. Sellars, J. Twamley, L.J. Brown, *et al.* Observation and control of blinking nitrogen-vacancy centres in discrete nanodiamonds. Nat. Nanotechnol., 5 (2010), pp. 345-349, 10.1038/nnano.2010.56

[24] B.R. Smith, D.W. Inglis, B. Sandnes, J.R. Rabeau, A.V. Zvyagin, D. Gruber, *et al.* Five-nanometer diamond with luminescent nitrogen-vacancy defect centers. Small, 5 (2009), pp. 1649-1653, 10.1002/smll.200801802

[25] C. Kurtsiefer, S. Mayer, P. Zarda, H. Weinfurter. Stable solid-state source of single photons

Phys. Rev. Lett., 85 (2000), pp. 290-293, 10.1103/PhysRevLett.85.290

[26] A. Khalid, K. Chung, R. Rajasekharan, D.W.M. Lau, T.J. Karle, B.C. Gibson, *et al.* Lifetime reduction and enhanced emission of single photon color centers in nanodiamond via surrounding refractive index modification. Sci. Rep., 5 (2015), 10.1038/srep11179

[27] C.-H. Su, A.D. Greentree, L.C.L. Hollenberg. Towards a picosecond transform-limited nitrogen-vacancy based single photon source. Opt. Express, 16 (2008), p. 6240, 10.1364/OE.16.006240

[28] A. Albrecht, A. Retzker, F. Jelezko, M.B. Plenio. Coupling of nitrogen vacancy centres in nanodiamonds by means of phonons. New J. Phys., 15 (2013), p. 083014, 10.1088/1367-2630/15/8/083014

[29] Q. Zhang, X. Liu, M.I.B. Utama, J. Zhang, M. de la Mata, J. Arbiol, *et al.* Highly enhanced exciton recombination rate by strong electron–phonon coupling in single ZnTe nanobelt. Nano Lett., 12 (2012), pp. 6420-6427, 10.1021/nl3037867

[30] S. Stehlik, T. Petit, H.A. Girard, A. Kromka, J.-C. Arnault, B. Rezek. Surface potential of diamond and gold nanoparticles can be locally switched by surrounding materials or applied voltage. J. Nanoparticle Res., 16 (2014), pp. 1-11, 10.1007/s11051-014-2364-8

[31] A.D. Greentree, B.A. Fairchild, F.M. Hossain, S. Prawer. Diamond integrated quantum photonics. Mater. Today., 11 (2008), pp. 22-31, 10.1016/S1369-7021(08)70176-7

[32] Y. Itoh, Y. Sumikawa, H. Umezawa, H. Kawarada. Trapping mechanism on oxygen-terminated diamond surfaces. Appl. Phys. Lett., 89 (2006), p. 203503, 10.1063/1.2387983

[33] E. Verveniotis, A. Kromka, B. Rezek. Controlling electrostatic charging of nanocrystalline diamond at nanoscale. Langmuir, 29 (2013), pp. 7111-7117, 10.1021/la4008312

[34] B. Rezek, C. Sauerer, C.E. Nebel, M. Stutzmann, J. Ristein, L. Ley, *et al.* Fermi level on hydrogen terminated diamond surfaces. Appl. Phys. Lett., 82 (2003), pp. 2266-2268, 10.1063/1.1564293

[35] D. Takeuchi, S. Yamanaka, H. Watanabe, H. Okushi. Device grade B-doped homoepitaxial diamond thin films. Phys. Status Solidi A., 186 (2001), pp. 269-280, 10.1002/1521-396X(200108)186:2<269::AID-PSSA269>3.0.CO;2-Z

[36] B. Rezek, C.E. Nebel. Kelvin force microscopy on diamond surfaces and devices. Diam. Relat. Mater., 14 (2005), pp. 466-469, 10.1016/j.diamond.2005.01.041.

[37] M. Tachiki, Y. Kaibara, Y. Sumikawa, M. Shigeno, H. Kanazawa, T. Banno, *et al.* Characterization of locally modified diamond surface using Kelvin probe force microscope. Surf. Sci., 581 (2005), pp. 207-212, 10.1016/j.susc.2005.02.054